

Effects of Phase Noise on OFDM Systems With and Without PLL: Characterization and Compensation

Denis Petrovic, *Member, IEEE*, Wolfgang Rave, and Gerhard Fettweis, *Senior Member, IEEE*

Abstract—In this paper, we propose an algorithm for suppressing intercarrier interference due to phase noise in coded orthogonal frequency division multiplexing (OFDM) systems. The algorithm approximates the phase-noise waveform by using a Fourier series approximation for the current phase-noise realization. Thereby, it cancels the effects of the phase noise beyond the standard common phase error correction used in contemporary OFDM standards. The algorithm requires that the correlation properties of the intercarrier interference are known. We calculate these properties in terms of the phase-noise spectral correlation matrix for both *Wiener* and *Ornstein–Uhlenbeck* phase-noise models, respectively. This modeling corresponds to a free-running oscillator, as well as a phase-locked loop realization of the local oscillator in orthogonal frequency division multiplexing transceivers. For both transceiver configurations, we investigate the performance of the proposed algorithm. It is demonstrated that the new algorithm achieves as much as one order of magnitude better performance in terms of packet/bit error rate when compared to a receiver with only the common phase error suppression.

Index Terms—Orthogonal frequency division multiplexing (OFDM), phase-locked loop, phase noise.

I. INTRODUCTION

TODAY, both broadcasting [digital video broadcast (DVB)] [1] and wireless local area networks (WLAN) within the family of 802.11 standards [2], adopt orthogonal frequency division multiplexing (OFDM) as the modulation type. As robust as OFDM systems are, e.g., to frequency selective fading, they are equally sensitive to synchronization errors, one of them being phase noise. Phase noise arises predominantly due to imperfections of the local oscillator (LO) in the transceiver. Essentially, it represents a time-varying drift of the LO phase from its reference.

Striving for higher spectral efficiency and data rate, solutions for the problem become even more relevant, as they allow the use of higher order modulation or the placement of subcarriers closer together. With recent advances in device technology, the use of higher frequency bands (20–60 GHz), where plenty of

Paper approved by S. K. Wilson, the Editor for Transmission Systems of the IEEE Communications Society. Manuscript received June 5, 2005; revised October 24, 2006 and November 20, 2006. This work was supported by the German Ministry of Research and Education within the project Wireless Gigabit with Advanced Multimedia (WIGWAM) under Grant 01 BU 370. This paper was presented in part at the 8th International OFDM Workshop 2003, the IEEE Vehicular Technology Conference Fall 2004, and the IEEE International Conference on Communications 2005.

D. Petrovic was with the Vodafone Chair for Mobile Communications, Dresden University of Technology, D-01062 Dresden, Germany; he is now with Rohde&Schwarz, Munich, Germany (e-mail: Denis.Petrovic@rsd.rohde-schwarz.com).

W. Rave and G. Fettweis are with the Vodafone Chair for Mobile Communications, Dresden University of Technology, D-01062 Dresden, Germany (e-mail: rave.ifn.et.tu-dresden.de; fettweis@ifn.et.tu-dresden.de).

Digital Object Identifier 10.1109/TCOMM.2007.902593

bandwidth is available, becomes an option [3] for WLAN. However, because the effect of a noisy oscillator grows quadratically with the carrier frequency, the phase noise becomes critical. Thus, knowing the effects of phase noise and keeping them below a certain level will play an important role in future wireless communication systems.

The influence of phase noise on OFDM has been extensively analyzed [4]–[10], starting with the SNR expressions for small angle phase noise in [4] or the investigation of the contributions of common phase error (CPE) and intercarrier interference (ICI) in [5]. More recently, a closed-form SINR expression for OFDM affected by phase noise together with a general phase-noise suppression algorithm was presented in [10] where a good overview of the problem is given.

In this paper, we want to go beyond the standard approach to compensate the CPE [10]–[12]. Our primary aim is to investigate the potential of an ICI suppression algorithm first described in [13] (a similar idea was described independently almost at the same time in [14], other approaches can be found in [15] and [16]).

Another question concerns the performance difference of OFDM receivers using free-running oscillators (phase noise modeled as a *Wiener* process that is usually studied in the literature) and receivers with a phase-locked loop (PLL) (*Ornstein–Uhlenbeck* process). Applying the techniques developed recently in [17] and [18] to OFDM transmission, we show for a system similar with 802.11a parameters that a better CPE correction can be achieved under the action of a feedback loop.

Taking this as a background, the present paper has the following objectives.

- 1) Propose and study the capability of the aforementioned ICI suppression algorithm, which estimates and corrects the phase-noise waveform using a truncated Fourier series in a decision feedback manner.
- 2) Provide an approach to characterize the intercarrier interference in terms of its correlation properties, which are required by the algorithm.
- 3) Compare the performance of phase-noise correction (CPE and/or ICI) in OFDM systems for *Wiener* and *Ornstein–Uhlenbeck* phase-noise models, representing free-running oscillators and PLLs, respectively.

The outline of the rest of the paper is as follows. Section II presents the system model followed by the phase-noise models for a free-running oscillator and a PLL in Section III. Section IV presents the iterative decision feedback algorithm for ICI suppression, which extends our previous work [13], [19], [20]. Because the algorithm requires the properties of ICI in terms of a spectral correlation matrix (of the phase-noise process), these are calculated in Section V.

In Section VI, we show that the iterative approach can significantly reduce error propagation as compared to correction in a single step used in our initial work and to pure CPE correction. Comparing the results for free-running oscillators and PLLs as a function of oscillator linewidth for additive white Gaussian noise (AWGN) and fading channels, we illustrate the performance gains relative to standard CPE correction.

II. SYSTEM MODEL

A. OFDM Transmission

We consider coded OFDM transmission, assuming a system with N subcarriers, carrier spacing Δf_{carr} , a bandwidth of W hertz and a sampling rate $T_s = 1/W$. Since OFDM transmission is block oriented, quadrature-amplitude modulation (QAM) symbols $X_k^{(m)}, k = 0, 1, \dots, N - 1$ to be transmitted within the m th OFDM symbol, are grouped into $(N \times 1)$ vectors $\mathbf{X}^{(m)} = [X_0^{(m)}, X_1^{(m)}, \dots, X_{N-1}^{(m)}]^T$. An inverse discrete-time Fourier transform on $\mathbf{X}^{(m)}$ gives a continuous time representation of the complex envelope of an OFDM symbol of duration $T = NT_s = 1/\Delta f_{\text{carr}}$ ¹

$$x^{(m)}(t) = \frac{1}{\sqrt{N}} \sum_{k=0}^{N-1} X_k^{(m)} e^{j2\pi kt/T} w(t) \quad (1)$$

where $w(t)$ denotes a rectangular window of height one and duration T . Subsequently, we focus on the discrete-time signal in the digital baseband obtained from (1) by sampling at time instants $t = nT/N = nT_s$

$$x_n = \frac{1}{\sqrt{N}} \sum_{k=0}^{N-1} X_k e^{j2\pi kn/N}, \quad n \in \{0, \dots, N - 1\}. \quad (2)$$

To allow simple one-tap equalization and to avoid interference among subsequent OFDM symbols, a so-called *cyclic prefix* or guard interval [21] of length G samples is prepended to a sampled envelope signal, resulting in a combined sequence $\mathbf{x}_{\text{tot}} = [x_{N-G}, \dots, x_{N-1}, x_0, \dots, x_{N-1}]$ of length $N_{\text{tot}} = N + G$ samples and duration $T_{\text{tot}} = T_{\text{CP}} + T$. The guard interval, the length of which is chosen to be a certain fraction of the signaling interval T , will be longer than the channel impulse response. This implies that there is no intersymbol interference within the window of N samples, and that the whole processing can be done in a symbol-by-symbol manner. For that reason, without loss of generality, we drop the OFDM symbol index m hereafter.

This sequence is upconverted to RF and transmitted through the channel, which is described by a time discrete impulse response $\mathbf{h} = [h_0, h_1, \dots, h_{L-1}]^T$ of duration LT_s . We assume that the channel estimates are ideal. Additionally, we assume

¹Throughout the paper, we use lower case letters for time-domain and upper case for frequency-domain values. Vectors and matrices are indicated with boldface and their components with subscripts, e.g., $\mathbf{X} = [X_0, X_1, \dots, X_{N-1}]^T$. The superscripts "T" and "H" at a vector/matrix indicate transpose and hermitian (conjugate transposition). For correlation matrices, subscripts indicate the quantities that are correlated with each other, while the arguments in brackets specify the relative shift, e.g., $\mathbf{R}_{i,j}(p, q)$. Finally, E denotes expectation, and the symbol \odot denotes circular convolution.

that the channel does not change during the transmission of one OFDM symbol. Although the analysis in this paper can be applied for any receiver architecture, for simplicity we adopt a direct conversion receiver [22], which means that both up- and downconversion are done in one step. Up- and downconversion oscillators are ideally harmonic functions of the form $x_{\text{osc}}^{\text{ideal}}(t) = e^{j2\pi f_c t}$ with carrier frequency f_c .

Phase noise is inherently present in oscillators, and its effect is equivalent to a random phase modulation of the carrier. Thus, the nonideal carrier signal has the form $x_{\text{osc}}^{\text{real}}(t) = e^{j2\pi f_c t + \phi(t)}$ with $\phi(t)$ as the random phase-noise process further discussed in Section III.

In general, phase noise is present at *both* the transmitter and the receiver, and has to be described as two multiplicative distortions together with the convolution by the channel impulse response [23]. However, for a small phase-noise bandwidth (relative to the subcarrier spacing, i.e., small total phase increment during one OFDM symbol), the resulting effect approximately equals that from the phase-noise process with a total bandwidth that is the sum of both the processes. We, therefore, restrict our discussion to the case with phase noise at the receiver only.²

B. OFDM Reception in the Presence of Receiver Phase Noise

In the ideal case, the transmitted symbols on all subcarriers $k = 0, 1, \dots, N - 1$ can be ideally recovered from the received signal samples. After removing the samples of the received signal which belong to the cyclic prefix, a discrete Fourier transform (DFT) operation is performed to the remaining samples. This leads to

$$R_k = \frac{1}{\sqrt{N}} \sum_{n=0}^{N-1} r_n e^{-j2\pi kn/N}. \quad (3)$$

The influence of phase noise on the received signal is most easily recognized by the following reasoning: Due to the cyclic prefix, the signal after the channel is equal to a circular convolution of the transmitted OFDM signal and the channel impulse response. Phase noise at the receiver affects the received signal as an angular *multiplicative* distortion in the time domain. Multiplication of two signals in the time domain is equivalent to convolving the spectra of the corresponding signals in the frequency domain.

To be precise, since discrete signals are considered here, in the frequency domain, the spectra of the two signals are *circularly* convolved [24]. The demodulated carrier amplitude R_k at subcarrier k is, therefore, obtained as [4], [9], [13]

$$\begin{aligned} \mathbf{r} &= \text{diag}(e^{j\Phi}) (\mathbf{x} \odot \mathbf{h}) \\ \mathbf{R} &= \mathbf{J} \odot (\mathbf{X}\mathbf{H}) \end{aligned} \quad (4)$$

²The model, therefore, directly applies to broadcasting applications, e.g., digital video broadcast (DVB), where the transmitter is of high quality while the mobile station is relatively cheap and of low quality. In case of WLAN applications where both access points and mobile stations are required to be cheap, the model could be used by doubling the assumed phase-noise bandwidth at the receiver assuming symmetry. We observed, indeed, that the proposed iterative correction performed almost identically when the phase-noise process was distributed equally between the transmitter and the receiver.

$$\Rightarrow R_k = X_k H_k \underbrace{J_0}_{\text{CPE}} + \underbrace{\sum_{l=0, l \neq k}^{N-1} X_l H_l J_{k-l}}_{\text{ICI}} + \eta_k. \quad (5)$$

The matrix $\text{diag}(e^{j\Phi})$ represents the current phase-noise realization $\Phi = [\phi_0 \dots \phi_{N-1}]$, X_k and H_k stand for the transmitted symbols and the sampled channel transfer function at subcarrier frequency k . The additive white noise η_k is unaffected in its statistical properties by the fast Fourier transform (FFT). The vector \mathbf{J} contains the DFT coefficients $J_i, i = -N/2, \dots, N/2 - 1$ of the current realization of the process $e^{j\Phi}$

$$J_i = \frac{1}{N} \sum_{n=0}^{N-1} e^{j\phi_n} e^{-j2\pi ni/N}. \quad (6)$$

The DC coefficient J_0 acts on all subcarriers as a common factor (5). In one OFDM symbol, it can be approximated for small phase noise as $J_0 \approx e^{j\bar{\phi}}$, where $\bar{\phi}$ corresponds to the mean rotation during that symbol. The common phase error must be corrected to obtain acceptable performance. This CPE correction is done by estimating the average rotation angle $\bar{\phi}$ during one OFDM symbol (typically using pilots) and derotating the demodulated amplitudes R_k after equalization, e.g., according to the methods described in [11] and [12].

III. PHASE-NOISE MODEL

In this section, we provide a summary of phase-noise models for two practical realizations of the LO, i.e., when the LO is realized as a free-running oscillator and as a PLL synthesizer. As in [17] and [25], to characterize carrier imperfections, we use a random carrier time shift $\alpha(t)$ rather than the phase shift $\phi(t)$. A noisy LO output signal is then described as $x_c(t + \alpha(t))$. Phase and time shift at the carrier frequency are related by $\phi(t) = 2\pi f_c \alpha(t)$.

A. Free-Running Oscillator

To describe the phase-noise process of a free-running oscillator, we employ the phase-noise model introduced in [17]. We summarize the most important results which we use for self-consistency as follows. The time shift $\alpha(t)$ is asymptotically (for large t) a *Wiener* or *Brownian* motion process

$$\alpha(t) = \sqrt{c}B(t) \quad (7)$$

where c is a parameter describing the oscillator quality. $B(t)$ stands for a standard *Wiener* process, i.e., an accumulated gaussian RV of unit variance $\mathcal{N}(0, 1)$. Because $B(t_2) - B(t_1) \propto \sqrt{|t_2 - t_1|} \mathcal{N}(0, 1)$, the variance of the Wiener process increases linearly with time, i.e., $\sigma_\alpha^2 = ct$ and the autocorrelation function of the process $\alpha(t)$ can be calculated as [17], [26]

$$E\{\alpha(t)\alpha(t + \tau)\} = c \min(t, t + \tau). \quad (8)$$

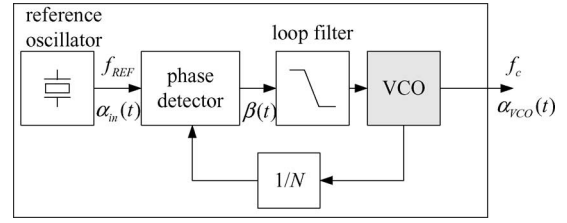


Fig. 1. Principal PLL components with the signals mentioned in the text.

In practice, the constant c is not directly available.³ Instead, a measure used to describe oscillator performance is the decay of the oscillator power spectral density around the first harmonic $\mathcal{L}(f_m)$ [dBc/Hz] [7], [17], where f_m is the frequency offset with respect to the carrier (oscillator) frequency f_c .

The connection between $\mathcal{L}(f_m)$ and c is achieved through the relation $\mathcal{L}(f_m) \approx 10 \log_{10} (cf_c^2/f_m^2)$ [17], which holds for f_m much larger than the phase noise 3-dB bandwidth, denoted by $\Delta f_{3\text{dB}}$. The relation between c and $\Delta f_{3\text{dB}}$ is given by $c = \Delta f_{3\text{dB}}/\pi f_c^2$ [17].

To characterize the phase-noise strength in OFDM transmission, we adopt a parameter widely used in the literature [4], which is the reduced or *relative* phase-noise bandwidth $\delta_{PN} = \Delta f_{3\text{dB}}/\Delta f_{\text{carr}}$.

B. PLL Synthesizer

In Fig. 1, the block diagram of the PLL together with time deviations at specific nodes of the PLL is shown. A negative feedback loop is closed around a low-quality voltage controlled oscillator (VCO). The frequency of the VCO is controlled through the phase detector (PD) and the low-pass filter (LPF) by the reference signal. Even though the reference signal stems from a very stable oscillator, this signal will, in reality, always feature a time deviation $\alpha_{in}(t)$ compared with the desired signal. As $\alpha_{in}(t)$ is at the output of the free-running oscillator, it is a *Wiener* process. The time deviation at the output of the PLL is denoted as $\alpha_{VCO}(t)$.

If one defines $\beta(t)$ as the time deviation at the input of the low-pass loop filter of the PLL, given as

$$\beta(t) = \alpha_{VCO}(t) - \alpha_{in}(t) \quad (9)$$

then, it is shown in [18] that $\alpha_{VCO}(t)$ is an *Ornstein-Uhlenbeck* process [26]. The correlation properties of $\alpha_{in}(t)$ and $\beta(t)$ are

$$E\{\beta(t_1)\alpha_{in}(t_2)\} = \sum_{i=1}^{n_o} \mu_i e^{\lambda_i \min(0, t_2 - t_1)} \quad (10)$$

$$E\{\beta(t_1)\beta(t_2)\} = \sum_{i=1}^{n_o} \nu_i e^{-\lambda_i |t_1 - t_2|} \quad (11)$$

respectively. The parameter $n_o = 1 + o_{lpf}$ represents the incremented order o_{lpf} of the loop filter within the PLL. A general

³In the existing literature, phase noise in OFDM is often described as a Brownian motion process $\phi(t)$ with variance $2\pi\beta t$, where $\beta = 2\Delta f_{3\text{dB}}$, i.e., the frequency spacing between the 3-dB points of the Lorentzian power spectral density. The connection between c and β is obtained through: $\sigma_\phi^2 = 2\pi\beta t = 4\pi^2 f_c^2 \sigma_\alpha^2 = 4\pi^2 f_c^2 ct \Rightarrow 4\pi\Delta f_{3\text{dB}} = 4\pi^2 f_c^2 c \Rightarrow \Delta f_{3\text{dB}} = \pi f_c^2 c$.

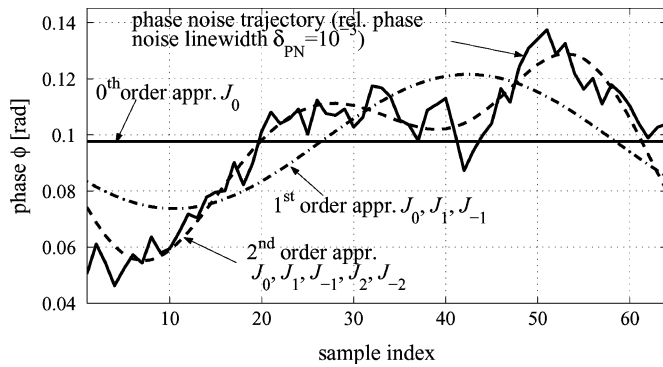


Fig. 2. Example of a phase-noise realization and its approximation using different orders of its current spectral components J_i .

algorithm is given in [18] to calculate all parameters of the PLL that are needed for its noise analysis, i.e., λ_i , μ_i , and ν_i . In Appendix B, closed-form expressions for the parameters of the exemplary charge pump PLL used throughout this paper can be found. These correlation properties will be used later in this paper. It is to be noted that the phase noise in this case is calculated as $\phi(t) = 2\pi f_c \alpha_{VCO}(t)$.

IV. PHASE-NOISE CORRECTION

In this section, we present an algorithm for ICI suppression whose basic idea is as follows: Phase-noise compensation beyond simple CPE correction will become possible if a reliable estimate of the instantaneous realization of the phase-noise process can be obtained. If several of the previously introduced DFT coefficients J_i (representing the spectral components of the current segment of the random process $e^{j\phi}$; see (6)) would be known, they could be used to provide this desired approximation of the current phase-noise realization. Additionally, because $e^{j\phi}$ has the characteristics of a low-pass signal (*Lorentzian* spectrum of the *Wiener* process), one can expect that only a few spectral components give a good approximation of such a phase-noise realization.

This concept is illustrated in Fig. 2 for the example of a free-running oscillator with relative phase-noise bandwidth $\delta_{PN} = 10^{-3}$. We see that including the terms J_i up to the second-order approximates the phase-noise realization much closer than the DC value alone corresponding to the standard CPE correction (0th order approximation).

Our proposed ICI cancelation algorithm should, thus, provide estimates of as many spectral components J_i , $i = -N/2, \dots, N/2 - 1$ as possible. The required J_i are hidden in the observed subcarrier symbols R_l , $l = 0, 1, \dots, N - 1$ at the output of the DFT demodulator [see (5)]. A trade off between reliable estimation and approximation order has to be found.

A. Estimation of the Spectral Components $J(i)$

The problem of estimating these Fourier coefficients up to a certain order can be recognized as a linear estimation problem [27, Ch. 10], [28]. A parameter vector (in our case, the coefficients J_i) disturbed by Gaussian noise due to the AWGN term and the remaining ICI beyond the estimation order has to be estimated.

To obtain this model, we rewrite (5) using a subset $L = \{l_1, l_2, \dots, l_P\}$ of reliably detected subcarrier symbols

$$\begin{bmatrix} R_{l_1} \\ R_{l_2} \\ \vdots \\ R_{l_P} \end{bmatrix} = \underbrace{\begin{bmatrix} A_{l_1} & \cdots & A_{l_1+u} \\ A_{l_2} & \cdots & A_{l_2+u} \\ \vdots & \vdots & \vdots \\ A_{l_P} & \cdots & A_{l_P+u} \end{bmatrix}}_{\mathbf{A}} \underbrace{\begin{bmatrix} J_0 \\ J_1 \\ J_{-1} \\ \vdots \\ J_u \\ J_{-u} \end{bmatrix}}_{\mathbf{J}_u} + \underbrace{\begin{bmatrix} \zeta_{ICI,l_1} \\ \zeta_{ICI,l_2} \\ \vdots \\ \zeta_{ICI,l_P} \end{bmatrix}}_{\zeta_{ICI}} + \underbrace{\begin{bmatrix} \eta_{l_1} \\ \eta_{l_2} \\ \vdots \\ \eta_{l_P} \end{bmatrix}}_{\boldsymbol{\eta}}. \quad (12)$$

It is to be noted that for the product $R_k H_k$ we used A_k as an abbreviation. The set L , taken from the whole set of carrier indices $\{0, 1, \dots, N - 1\}$, has to be of cardinality at least $2u + 1$ to solve for the desired number of unknowns at estimation order u .

Finally, we rewrite (12) in compact form as

$$\mathbf{R} = \mathbf{A}\mathbf{J}_u + \boldsymbol{\varepsilon} \quad (13)$$

where $\boldsymbol{\varepsilon} = \zeta_{ICI} + \boldsymbol{\eta}$ represents the effective measuring noise that combines the AWGN contribution plus the residual ICI beyond the current estimation order u .

The system model represented by (13) is a linear model with respect to the vector \mathbf{J}_u , and we choose the minimum mean square estimation (MMSE) to estimate this vector from the demodulated received symbols vector \mathbf{R} .

The MMSE estimate [28] of the vector \mathbf{J}_u is given by

$$\hat{\mathbf{J}}_u = \mathbf{M}\mathbf{R} \quad (14)$$

with the filtering matrix

$$\mathbf{M} = \mathbf{R}_{J_u J_u} \mathbf{A}^H (\mathbf{A} \mathbf{R}_{J_u J_u} \mathbf{A}^H + \mathbf{R}_{\boldsymbol{\varepsilon}\boldsymbol{\varepsilon}})^{-1} \quad (15)$$

where $\mathbf{R}_{J_u J_u}$ and $\mathbf{R}_{\boldsymbol{\varepsilon}\boldsymbol{\varepsilon}}$ represent the correlation matrices of \mathbf{J}_u and $\boldsymbol{\varepsilon}$, respectively. The estimation of \mathbf{J}_u assumes knowledge of one part of the transmitted symbols apart from the channel knowledge. This knowledge is obtained in a decision feedback (DF) manner as described in Section IV-B. The detailed calculation of the correlation matrices $\mathbf{R}_{J_u J_u}$ and $\mathbf{R}_{\boldsymbol{\varepsilon}\boldsymbol{\varepsilon}}$ is presented in Section V.

B. ICI Correction Algorithm

Now, we are in the position to present our ICI suppression algorithm, which can be performed once the DFT coefficients are known. Phase noise suppression in the time domain would be a logical approach. One should multiply samples of the received signal (after the removal of the cyclic prefix) r_n , $n = 0, 1, \dots, N - 1$ with the estimate of $e^{-j\phi_n}$. However, to avoid additional FFT operations, multiplication in the time domain for discrete-time systems can be mapped to a circular convolution of the involved DFT spectra in the frequency

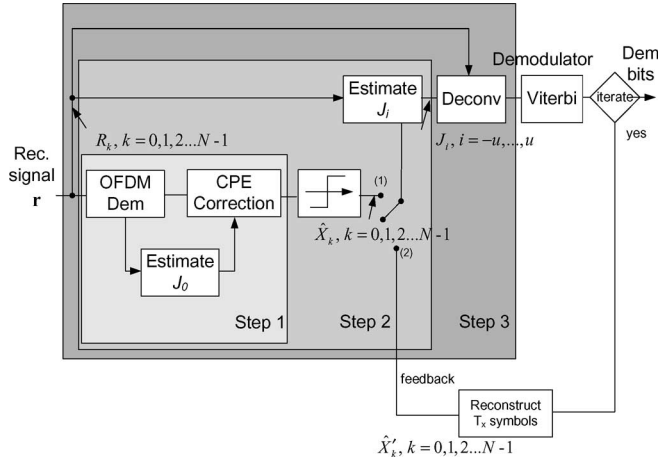


Fig. 3. Block diagram of the iterative phase-noise suppression algorithm.

domain. As we estimate only a small number of phase-noise DFT coefficients (the rest is assumed to be zero), the computational complexity of the deconvolution can be significantly reduced.

In our case, this means that ICI cancellation for one OFDM symbol in the frequency domain can be done by circularly convolving the vector of the demodulated symbols of all subcarriers $\mathbf{R} = [R_0, \dots, R_{N-1}]^T$ with the vector of the estimated DFT coefficients of the vector $e^{-j\phi}$. Using the properties of the DFT (see, e.g., [24]), if $\hat{\mathbf{J}} = \text{DFT}\{e^{j\phi}\}$, the spectrum of the complex conjugate signal $e^{-j\phi}$ ($\mathbf{U} = \text{DFT}\{e^{-j\phi}\}$) reads $U_i = \hat{J}_{-i}^*$, $i = -N/2, \dots, N/2 - 1$.

Therefore, ICI suppression in the frequency domain can be realized by circularly convolving the vectors \mathbf{R} and \mathbf{U} to obtain the corrected vector of subcarrier symbols $\hat{\mathbf{R}}_N$

$$\hat{\mathbf{R}}_N = \mathbf{R}_N \odot \hat{\mathbf{U}}. \quad (16)$$

The main task of the algorithm, thus, consists in estimating the DFT components of the current phase-noise realization and in suppressing the ICI by performing a deconvolution in the frequency domain. It can be summarized as follows (see the block diagram in Fig. 3).

- *Step 1:* Use standard OFDM demodulation to obtain an estimate \hat{J}_0 of J_0 using one of the approaches for CPE estimation [11], [12] to derotate the demodulated signal constellation.
- *Step 2:* Using such a derotated constellation, make a decision on the transmitted symbols and use these hard decisions for the estimation of the \hat{J}_i , $i = -u, \dots, u$, according to the method provided in Section IV-A.
- *Step 3:* The estimated DFT coefficients \hat{J}_i , $i = -u, \dots, u$ comprise the vector $\hat{\mathbf{J}}$. All terms \hat{J}_i , $|i| > u$ that are not estimated are set to be zero. The vector $\hat{\mathbf{U}}$ of the estimated DFT coefficients of $e^{-j\phi}$ can then be formed as described earlier in this section.

The demodulated symbols with suppressed ICI up to order u are obtained as $\hat{\mathbf{R}}_N = \mathbf{R}_N \odot \hat{\mathbf{U}}$.

After the first iteration, instead of hard decisions based on the initial CPE correction, symbol estimates after decoding are used to improve the estimate of the DFT coefficients \hat{J}_i .

C. Iterative Phase-Noise Suppression

An increasing number of reliable symbols, which are used for phase-noise estimation, will improve the quality of the phase-noise estimation and, thus, the quality of the phase-noise suppression. This can be achieved if the algorithm proposed in Section IV-B is applied iteratively, meaning that the transmitted symbols are reconstructed after phase-noise correction and used again for a consecutive phase-noise estimation and correction (see Fig. 3).

A further refinement would be to use soft output from a MAP decoder to find the reliable transmitted symbols [20] for the next iteration. In this paper, we avoid this additional complexity and use standard Viterbi decoding, selecting the subset of subcarriers used for phase-noise estimation from the strongest channels and their neighboring channels.

V. PROPERTIES OF ICI

In order to be able to calculate the filtering matrix in (15), the correlation properties of the vectors \mathbf{J}_u (the Fourier coefficients of the phase noise up to order u) and ε (the remaining noise due to ICI plus AWGN) have to be calculated. These are given by the correlation matrices $\mathbf{R}_{J_u J_u}$ and $\mathbf{R}_{\varepsilon \varepsilon}$, respectively.

An important difference of our analysis [19], [29] to previous approaches [9], [30], [31] is that we consider the signal $e^{j\phi(t)}$ rather than the phase $\phi(t)$. The advantage of this kind of approach is that even if $\phi(t)$ is nonstationary with undefined spectrum (e.g., a *Wiener* process), the signal $e^{j\phi(t)}$, in contrast, is stationary and has a well-defined spectrum [17].

A. Phase-Noise Spectral Correlation Matrix

Our starting point is the vector $\mathbf{J} = [J_{-N/2} \dots J_{N/2-1}]^T$ of DFT coefficients of one realization of $e^{j\phi_n}$ during one OFDM symbol, as given by (6). The correlation matrix of this vector is defined as $\mathbf{R}_{J,J} = E\{\mathbf{J}\mathbf{J}^H\}$. Using (6), the (p, q) th element of the correlation matrix $\mathbf{R}_{J,J}$ is calculated as

$$\begin{aligned} \mathbf{R}_{J,J}(p, q) &= E\{J_p J_q^*\} \\ &= \frac{1}{N^2} E \left\{ \sum_{k=0}^{N-1} \sum_{l=0}^{N-1} e^{j(\phi_k - \phi_l)} e^{-j\frac{2\pi}{N}(pk - ql)} \right\} \\ &= \frac{1}{N^2} \sum_{k=0}^{N-1} \sum_{l=0}^{N-1} E \{ e^{j\Delta\phi_{kl}} \} e^{-j\frac{2\pi}{N}(pk - ql)}. \end{aligned} \quad (17)$$

In order to evaluate (17), the expectation $E\{e^{j\Delta\phi_{kl}}\}$ has to be calculated for each parameter pair $k, l \in \{0, 1, \dots, N-1\}$.

Using the characteristic function ψ_{kl} of the random variable $\Delta\phi_{kl}$ defined as $\psi_{kl}(\omega) = E\{e^{j\omega\Delta\phi_{kl}}\}$, one recognizes that $E\{e^{j\Delta\phi_{kl}}\} = \psi_{kl}(\omega = 1)$. Thus, it follows that the desired autocorrelation coefficients equal the two-dimensional discrete-time Fourier transform [24] of $\psi_{kl}(1)$, ($k, l \in \{0, 1, \dots, N-1\}$)

$$\begin{aligned} \mathbf{R}_{J,J}(p, q) &= E\{J_p J_q^*\} \\ &= \frac{1}{N^2} \sum_{k=0}^{N-1} \sum_{l=0}^{N-1} \psi_{kl}(1) e^{-j\frac{2\pi}{N}(pk - ql)}. \end{aligned} \quad (18)$$

Therefore, if $\psi_{kl}(1)$, $k, l = 0, 1, \dots, N-1$ is known, the elements of the correlation matrix \mathbf{R}_{JJ} can be calculated using (18).

Using the work of [17] and [18], the characteristic function $\psi_{kl}(1)$ for the two practical cases of interest, i.e., for a free-running oscillator and for the frequency synthesizer realized by a PLL, can be expressed in closed form (more details on these expressions can be found in Appendix I-A and in [17], [18]).

1) Free-running oscillator

$$E \{ e^{j\Delta\phi_{kl}} \} = e^{-\frac{\omega_c^2 c |k-l| T_s}{2}}. \quad (19)$$

2) PLL synthesizer

$$E \{ e^{j\Delta\phi_{kl}} \} = e^{-\frac{\omega_c^2}{2} \left(c_{in} |k-l| T_s + 2 \sum_{i=1}^{n_o} (\mu_i + \nu_i) \left(1 - e^{-\lambda_i |k-l| T_s} \right) \right)}. \quad (20)$$

B. ICI Power

Consider again the ICI sum in (5). The correlation between the DFT coefficients J_i , if any, is destroyed due to the randomization by data symbols and channel coefficients. Assuming that $E\{X_k X_l^*\} = E_s \delta(k-l)$, where $\delta(\cdot)$ denotes the Kronecker impulse and $E\{H_k^2\} = 1$, the total ICI power can be calculated as

$$\begin{aligned} \sigma_{ICI}^2 &= E \left\{ \left| \sum_{\substack{l=-N/2 \\ l \neq 0}}^{N/2-1} X_{k-l} H_{k-l} J_l \right|^2 \right\} \\ &= \sum_{\substack{l=-N/2 \\ l \neq 0}}^{N/2-1} E\{|X_{k-l}|^2\} E\{|H_{k-l}|^2\} E\{|J_l|^2\} \\ &= E_s \sum_{\substack{l=-N/2 \\ l \neq 0}}^{N/2-1} E\{|J_l|^2\} = E_s [1 - E\{|J_0|^2\}]. \quad (21) \end{aligned}$$

It means that the ICI power can be calculated either via the power of the DC term of the phase-noise spectrum or by summing all other components. This can be understood intuitively from the principle of energy conservation (a derivation of this result in slightly more general form than in [4] can be found in the appendix).

It is to be noted that the ICI power can be calculated as the trace or sum of the diagonal elements of the correlation matrix \mathbf{R}_{JJ} calculated earlier excluding the term $E\{|J_0|^2\}$ according to (21)

$$\sigma_{ICI}^2 = \text{tr}(\mathbf{R}_{JJ}) - \mathbf{R}_{JJ}(0, 0). \quad (22)$$

C. Calculation of $\mathbf{R}_{J_u J_u}$ and $\mathbf{R}_{\varepsilon\varepsilon}$

Finally, the correlation matrix $\mathbf{R}_{J_u J_u}$, which is required for estimation of the vector \mathbf{J}_u (see Section IV-A), is evaluated by selecting the required columns and rows of \mathbf{R}_{JJ} , the evaluation of which is described in (21).

In addition, assuming that the data symbols are uncorrelated, the correlation matrix $\mathbf{R}_{\varepsilon\varepsilon}$ of the remaining noise terms in the

MMSE estimator is given by

$$\mathbf{R}_{\varepsilon\varepsilon} = \text{diag}(E\{|\zeta_{l_1}|^2\} + \sigma_n^2, \dots, E\{|\zeta_{l_P}|^2\} + \sigma_n^2). \quad (23)$$

Here, $E\{|\zeta_{l_i}|^2\}$ denotes the power of the residual (nonestimated) ICI on subcarrier ζ_{l_i} . Using (5) and (13), the terms $\zeta(l_i)$ and $l_i \in L$ can be expressed as

$$\zeta_{l_i} = \sum_{\substack{\nu=-N/2 \\ |\nu| > u}}^{N/2-1} X_{l_i-\nu} H_{l_i-\nu} J_\nu. \quad (24)$$

The power of the ζ_{l_i} is calculated similarly as the total ICI power in (21) using the diagonal elements $E\{|J_\nu|^2\}$ of the matrix \mathbf{R}_{JJ} beyond the estimation order

$$E\{|\zeta_{l_i}|^2\} = \sum_{\substack{\nu=-N/2 \\ |\nu| > |u|}}^{N/2-1} E\{|J_\nu|^2\}.$$

VI. CASE STUDIES WITH NUMERICAL RESULTS

To investigate the performance of the proposed algorithms, we resort to Monte Carlo simulations. System parameters correspond to the IEEE 802.11a Standard [2], i.e., 48 useful carriers, four pilot symbols that we use for initial CPE correction, 64 QAM with gray mapping, and a half-rate convolutional code of memory six. One codeword spanned three OFDM symbols equalling a packet. Within the simulations, six phase-noise correction schemes are compared:

- 1) without phase noise;
- 2) phase noise with ideal CPE correction (ICPE);
- 3) phase noise with CPE correction using the least squares (LS) algorithm according to [12];
- 4) phase noise and genie ICI correction of order $u = 3$;
- 5) one-step ICI correction of order $u = 3$ with initial CPE correction as in [12]; and
- 6) phase noise and iterative ICI correction of increasing correction order up to $u = 3$ with initial CPE correction as in [12].

We investigate the performance of these different correction schemes for both AWGN and frequency selective channels. Starting with the AWGN channel and a free-running oscillator (see Fig. 4), we plot as performance criterion the increase of the packet error rate (PER) as a function of relative oscillator linewidth δ_{PN} , either at that SNR value for which without phase noise a typical target value of $\text{PER} = 10^{-2}$ is achieved (SNR = 18.6 dB in case of coded 64-QAM transmission) or the SNR loss relative to that value.

Although *noniterative* ICI correction shows better performance than CPE correction alone, the results are significantly worse than those that could be achieved with genie symbol detection and ICI correction of the same specified order. Obviously, falsely detected symbols used to estimate the phase-noise DFT coefficients in Step 2 of the noniterative algorithm deteriorate the estimation result. This problem becomes more pronounced for a larger phase-noise bandwidth for which ICI increases together with the CPE estimation error.

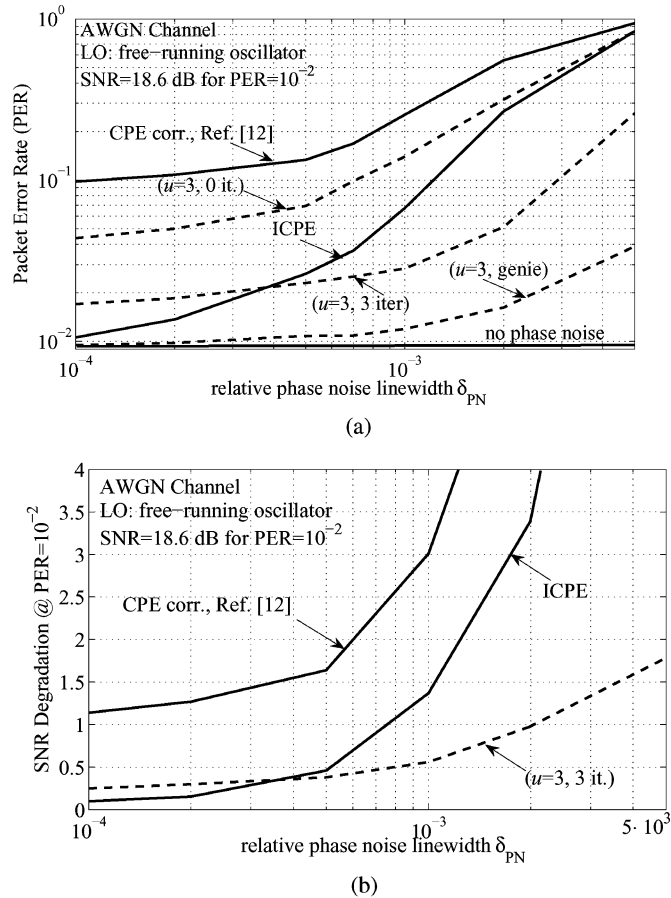


Fig. 4. Performance of the phase-noise suppression algorithms over an AWGN channel and systems with LO realized as a free-running oscillator as a function of the relative phase-noise bandwidth δ_{PN} . (a) PER degradation relative to PER = 10^{-2} without phase noise at SNR = 18.6 dB: AWGN channel for different correction methods. (b) SNR loss relative to PER = 10^{-2} without phase noise: Standard and ideal CPE correction *versus* iterative ICI correction.

To reduce this error propagation problem, iterative processing turns out to be appropriate. A more gradual reconstruction of the phase-noise realization is able to correct many residual errors, and provides results that are roughly an order of magnitude better than pure CPE correction. As can be seen in Fig. 4(a), the curves for conventional CPE correction and iterative third-order ICI correction run almost in parallel as a function of oscillator linewidth. A further increase of the approximation order did not improve the performance for our parameters (for a larger number of subcarriers where more choices to select reliable neighbourhoods of subcarriers exist, this could be different). For comparison, the SNR loss for achieving a PER of 10^{-2} relative to the reference value of 18.6 dB without phase noise on the AWGN is plotted in Fig. 4(b).

Similar results and comments as for the case of a free-running oscillator apply to a PLL with respect to the performance of iterative and noniterative ICI correction (not shown for the AWGN). We, thus, turn immediately to the performance of the algorithms over frequency selective channels illustrated for the example of an ETSI A channel in Fig. 5(b) that compares free-running os-

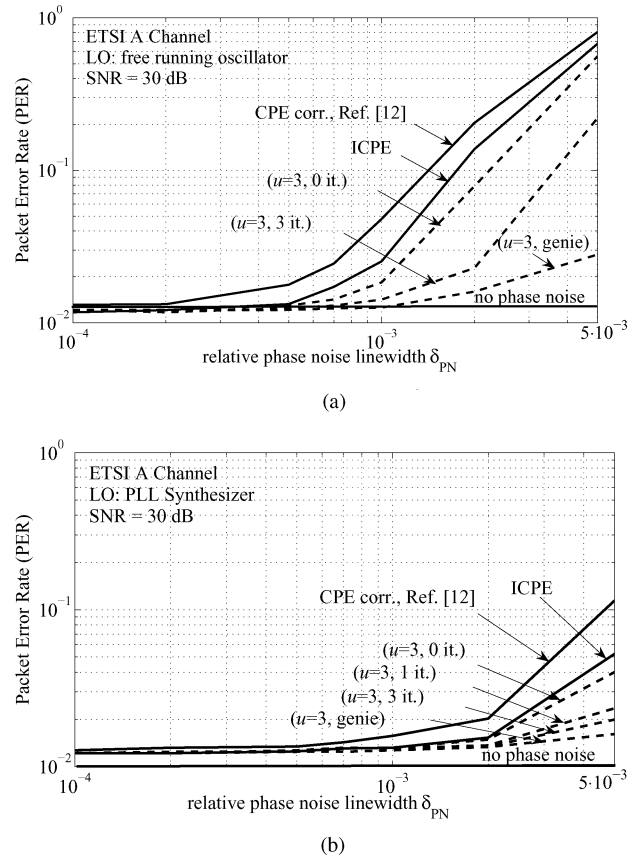


Fig. 5. Performance of phase-noise suppression for a fading channel. (a) PER degradation relative to PER = 10^{-2} without phase noise at SNR = 30 dB for an ETSI A channel for different correction methods for a free-running oscillator. (b) PER degradation for the same conditions as in (a) with a PLL synthesizer.

cillators and PLL synthesizers.⁴ It is to be noted that the SNR to achieve the target PER of 10^{-2} is much higher (30 dB) than on the AWGN. Also, the sensitivity to phase noise gets more pronounced because subcarriers in a fade get coupled to stronger adjacent carriers (thus, more DFT coefficients need to be used for compensation).

The effect of the PLL is twofold. First, it reduces the CPE because it limits the excursions of the phase-noise process that drift in a single direction (for a linear phase drift, the DFT coefficients decay only with $1/u$). This presumably is the most difficult case for ICI correction. As a consequence, the ICI correction algorithm has better starting conditions and works well with a lower correction order. Therefore, the strong rise of the packet error starts at a notably larger oscillator linewidth when the charge-pump PLL is used (roughly a factor of 5 larger than for the free-running oscillator; compare Fig. 5(a) and (b)).

A further comment applies to the useful number of iterations. We observed that the PER benefits more than the BER from the proposed ICI correction schemes for the following reason: If many subcarriers of one OFDM symbol are erroneously detected after the initial CPE correction, the subsequent ICI correction

⁴Each value in the plots represents at least several hundreds of transmitted packets with an independent realization of the channel model that did not change during the packet.

may even increase the number of errors within one packet, and these errors will propagate to the next iterations. If, however, the number of erroneous subcarriers after the first CPE correction is small, the phase-noise waveform will be reasonably approximated. This means that the ICI suppression algorithm can, with high probability, reduce the number of errors. This, in turn, will give an even better phase-noise approximation and let the corrections converge to an error-free packet. On the other hand, for low SNR, the bit error rate (BER) can even worsen with an increasing number of iterations or correction order (as is typical for decision feedback schemes).

The sensitivity of a system to phase noise and the performance of phase-noise suppression algorithms do not depend only on the transmission system itself, but also on the type of channel, i.e., the channel transfer function [19]. It is noteworthy that for AWGN channels and CPE estimation only [see Fig. 4(a)] the PER degrades significantly already for very small δ_{PN} . In our opinion, along with PER *versus* δ_{PN} type of figures, one should also plot the degradation of the SNR at some PER of interest (in our case, $\text{PER} = 10^{-2}$) as a function of a δ_{PN} . The reason for this is well seen at the example of the AWGN case. The PER *versus* SNR curves in this case are very steep, and thus, a PER degradation of one order of magnitude corresponds to a rather small SNR degradation. For frequency-selective channels, the SNR loss may be not so strong because the slope of the BER/PER curves is much smaller, although in both cases, the SNR loss diverges when an error floor occurs. This should be kept in mind when judging the figures presented in this section.

VII. SUMMARY AND CONCLUSION

Based on accurate knowledge of the ICI correlation matrix, we presented an algorithm for estimating the DFT coefficients of the realizations of the segmented phase process $e^{j\phi(t)}$ in OFDM transmission. The central idea is the approximation of the phase-noise realization by a DFT series. We can simplify this approximation by using only the lower order coefficients that dominate the series. Once we have them, we can use them to correct ICI in an iterative way.

Performance results for a WLAN scenario with AWGN and fading channels as a function of oscillator linewidth show that the algorithm can outperform conventional CPE correction by about one order of magnitude. A detailed comparison with the behavior of a PLL, which to the knowledge of the authors was not yet available in the literature so far, showed similar relations between the different correction schemes with advantages for the receiver with PLL. The latter predominantly filters the low-frequency part of the phase-noise spectrum, which makes CPE correction easier and gives a better start for ICI correction. To summarize, our proposed algorithm should allow either less pure (cheaper) oscillators or a smaller subcarrier spacing, which is of interest for longer channel impulse responses. As the complexity of the algorithm is certainly not negligible, a trade-off between complexity (number of iterations, correction order) and performance has to be found. One to three orders beyond CPE correction alone appear reasonable. This paper shows a step further in achieving the "dirty RF paradigm" [32] to com-

bine the signal processing in baseband with knowledge about the RF impairments.

APPENDIX I

A. Autocorrelation Properties of the Process $e^{j\phi(t)}$

The autocorrelation of this process can be found by the reasoning for obtaining the spectrum of a random process in [17] and [18]. Define $x_{\text{osc}}^{\text{real}}(t) = e^{j\omega_c \alpha(t)}$, where $\omega_c = 2\pi f_c$ and $\alpha(t)$ as the stochastic time shift of the output oscillator signal. The autocorrelation function $R(t, \tau)$ of the random process $x_{\text{osc}}(t)$, which needs to be calculated, is defined as

$$\lim_{t \rightarrow \infty} E \left\{ e^{j\omega_c (\alpha(t) - \alpha(t+\tau))} \right\} = e^{j\omega_c \mu(t) - \frac{\omega_c^2 \sigma^2(t, \tau)}{2}}$$

where the terms $\mu(t)$ and $\sigma^2(t, \tau)$ represent mean and variance of the process $(\alpha(t) - \alpha(t + \tau))$. It is to be noted that the autocorrelation function in this case is also the characteristic function of the random variable $\alpha(t) - \alpha(t + \tau)$ at the angular frequency ω_c^2 .

1) *Free-Running Oscillator*: The properties of $\alpha(t)$ for a free-running oscillator are given by (7) and (8). Next, consider the statistics of $\alpha(t) - \alpha(t + \tau)$ in order to evaluate the function $R(t, \tau)$ above, for $t \rightarrow \infty$. It is easy to show that

$$\lim_{t \rightarrow \infty} E \{ \alpha(t) - \alpha(t + \tau) \} = 0 \quad \text{and}$$

$$\lim_{t \rightarrow \infty} E \{ (\alpha(t) - \alpha(t + \tau))^2 \} = c\tau - 2\min(0, \tau) = c|\tau|.$$

Also, $\alpha(t) - \alpha(t + \tau)$ is asymptotically Gaussian, which means that its asymptotic characteristic function is

$$\lim_{t \rightarrow \infty} E \{ e^{j\omega_c (\alpha(t) - \alpha(t+\tau))} \} = e^{-\frac{\omega_c^2 c |\tau|}{2}}.$$

This provides the expectation required to calculate $R(\tau) = \lim_{t \rightarrow \infty} R(t, \tau)$. From the above arguments, it can be derived that the characteristic function of $\Delta\phi_{kl}$ for a free-running oscillator can be expressed as

$$E \{ e^{j\Delta\phi_{kl}} \} = e^{-\frac{\omega_c^2 c |k-l| T_s}{2}}$$

where $\Delta\phi_{kl}$ is the cumulative phase-noise increment between samples l and k of the received signal given as $\Delta\phi_{kl} = \omega_c (\alpha(kT_s) - \alpha(lT_s))$, and T_s is the sampling interval.

2) *PLL Synthesizer*: First, we note that

$$\mu(t) = \lim_{t \rightarrow \infty} (\alpha_{\text{VCO}}(t) - \alpha_{\text{VCO}}(t + \tau)) = 0.$$

Further, we have

$$\begin{aligned} \sigma^2(t, \tau) &= \lim_{t \rightarrow \infty} E \left\{ (\alpha_{\text{VCO}}(t) - \alpha_{\text{VCO}}(t + \tau))^2 \right\} \\ &= \lim_{t \rightarrow \infty} E \{ \alpha_{\text{VCO}}^2(t) \} + \lim_{t \rightarrow \infty} E \{ \alpha_{\text{VCO}}^2(t + \tau) \} \\ &\quad - 2 \lim_{t \rightarrow \infty} E \{ \alpha_{\text{VCO}}(t) \alpha_{\text{VCO}}(t + \tau) \}. \end{aligned}$$

Using (8)–(11), one can show that [18]

$$\sigma^2(t, \tau) = c_{in} |\tau| + 2 \sum_{i=1}^{n_o} (\mu_i + \nu_i) \left(1 - e^{-\lambda_i |\tau|} \right)$$

which is independent of t . Therefore, the characteristic function of $\Delta\phi_{kl}$ for a controlled oscillator can be expressed as

$$E \{ e^{j\Delta\phi_{kl}} \} = e^{-\frac{\omega_c^2}{2} \left(c_{in} |k-l| T_s + 2 \sum_{i=1}^{n_o} (\mu_i + \nu_i) \left(1 - e^{-\lambda_i |k-l| T_s} \right) \right)}$$

B. PLL Parameters

Within this paper, we used a charge pump PLL of the first order for which the parameters are given in the following. The charge pump can be modeled by a linear transfer function of the form $H(s) = k_{pd} \frac{s + \omega_1}{s}$, with zero frequency ω_1 and phase detector gain k_{pd} . To evaluate (10) and (11), the following parameters are required:

$$\lambda_{1,2} = \frac{\omega_1 \pm \sqrt{\omega_1^2 - 8\omega_1 \pi B_{PLL}}}{2}$$

$$\mu_1 = -\frac{c_{in}}{(\lambda_1 - \lambda_2)}, \quad \mu_2 = \frac{c_{in}}{(\lambda_2 - \lambda_1)}$$

$$\nu_1 = \frac{c_{in} + c_{VCO}}{(\lambda_1 - \lambda_2)^2} \left(\frac{\lambda_1}{2} - \frac{\lambda_1 \lambda_2}{\lambda_1 + \lambda_2} \right)$$

$$\nu_2 = \frac{c_{in} + c_{VCO}}{(\lambda_1 - \lambda_2)^2} \left(\frac{\lambda_2}{2} - \frac{\lambda_1 \lambda_2}{\lambda_1 + \lambda_2} \right).$$

B_{PLL} represents the bandwidth of the PLL. Since the order of the filter is $o_{pf} = 1$, we have $n_o = 1 + o_{pf} = 2$ in this case. In the original reference [18], PLL parameters are also calculated for other loop filters without a charge pump.

C. Relation Between CPE and ICI Power

An interesting property of the ICI coefficients that can be intuitively expected is the fact that it just represents that part of the received symbol energy that is not contained in the symbols purely affected by a common rotation. We remark that the following relation is the same as the one derived in [4] for a continuous phase-noise model, apart from the fact that we drop the assumption $N \rightarrow \infty$, thus, obtaining the validity of the result for a single OFDM symbol already.

First, we note that due to the periodicity property of the DFT coefficients of the phase noise, $\sum_{i=-N/2}^{N/2-1} E\{|J_i|^2\} = \sum_{i=0}^{N-1} E\{|J_i|^2\}$ holds. Using (6) and the periodicity property of the ICI coefficients, one finds

$$\sum_{i=-N/2}^{N/2-1} E\{|J_i|^2\} = \sum_{i=0}^{N-1} E\{J_i J_i^*\}$$

$$= \sum_{i=0}^{N-1} \frac{1}{N^2} \sum_{k=0}^{N-1} \sum_{l=0}^{N-1} E \left\{ e^{j(\phi(k) - \phi(l))} \right\} e^{-j\frac{2\pi}{N} i(k-l)}$$

$$= \frac{1}{N^2} \sum_{k=0}^{N-1} \sum_{l=0}^{N-1} E \left\{ e^{j\Delta\phi_{kl}} \right\} \sum_{i=0}^{N-1} e^{-j\frac{2\pi}{N} i(k-l)}$$

where $\Delta\phi_{kl}$ denotes the cumulative phase-noise increment between samples l and k of the received signal. Using the orthog-

onality identity of discrete complex exponentials [24]

$$\frac{1}{N} \sum_{v=0}^{N-1} e^{-j\frac{2\pi}{N} v(k-l)} = \delta_{k,l}$$

the above summation is evaluated as

$$\sum_{i=-N/2}^{N/2-1} E\{|J_i|^2\} = 1$$

noting that for $k = l$, $\Delta\phi_{kl} = 0$ and $e^{j\Delta\phi_{kl}} = 1$. The last property can be used to obtain the power of the ICI using the power of the dc coefficient of the phase-noise process as

$$\sigma_{ICI}^2 = E_s [1 - E\{|J_0|^2\}].$$

REFERENCES

- [1] H. Sari, G. Karam, and I. Jeanclaude, "Transmission techniques for digital terrestrial TV broadcasting," *IEEE Commun. Mag.*, vol. 33, no. 2, pp. 100–109, Feb. 1995.
- [2] *Part 11: Wireless LAN medium access control (MAC) and physical layer (PHY) specifications. High-speed physical layer in the 5 GHz band* IEEE Standard 802.11a-1999, 1999.
- [3] J. D. Cressler, "SiGe HBT technology: A new contender for Si-based RF and microwave circuit applications," *IEEE Trans. Microw. Theory Tech.*, vol. 46, no. 5, pp. 572–589, May 1998.
- [4] T. Pollet, M. V. Bladel, and M. Moeneclaey, "BER sensitivity of OFDM systems to carrier frequency offset and Wiener phase noise," *IEEE Trans. Commun.*, vol. 43, no. 2, pp. 191–193, Feb. 1995.
- [5] J. Stott, "The effects of phase noise in OFDM," *EBU Tech. Rev.*, Jul. 1998.
- [6] H. Steendam, M. Moeneclaey, and H. Sari, "The effect of carrier phase jitter on the performance of orthogonal frequency-division multiple-access systems," *IEEE Trans. Commun.*, vol. 46, no. 4, pp. 456–459, Apr. 1998.
- [7] A. Armada, "Understanding the effects of phase noise in orthogonal frequency division multiplexing (OFDM)," *IEEE Trans. Broadcast.*, vol. 47, no. 2, pp. 153–159, Jun. 2001.
- [8] M. S. El-Tanany, Y. Wu, and L. Hazy, "Analytical modeling and simulation of phase noise interference in OFDM-based digital television terrestrial broadcasting systems," *IEEE Trans. Broadcast.*, vol. 47, no. 3, pp. 20–31, Mar. 2001.
- [9] E. Costa and S. Pupolin, "M-QAM-OFDM system performance in the presence of a nonlinear amplifier and phase noise," *IEEE Trans. Commun.*, vol. 50, no. 3, pp. 462–472, Mar. 2002.
- [10] S. Wu and Y. Bar-Ness, "OFDM systems in the presence of phase noise: Consequences and solutions," *IEEE Trans. Commun.*, vol. 52, no. 11, pp. 1988–1996, Nov. 2004.
- [11] P. Robertson and S. Kaiser, "Analysis of the effects of phase noise in OFDM systems," in *Proc. ICC*, 1995.
- [12] S. Wu and Y. Bar-Ness, "A phase noise suppression algorithm for OFDM-based WLANs," *IEEE Commun. Lett.*, vol. 6, no. 12, pp. 535–537, Dec. 2002.
- [13] D. Petrovic, W. Rave, and G. Fettweis, "Phase noise suppression in OFDM including intercarrier interference," in *Proc. Int. OFDM Workshop*, 2003, pp. 219–224.
- [14] S. Wu and Y. Bar-Ness, "A new phase noise mitigation method in OFDM systems with simultaneous CPE and ICI correction," in *Proc. MCSS, Oberpfaffenhofen, Germany*, Sep. 2003.
- [15] R. A. Casas, S. Biracree, and A. Youtz, "Time domain phase noise correction for OFDM signals," *IEEE Trans. Broadcast.*, vol. 48, no. 3, pp. 230–236, Sep. 2002.
- [16] F. Munier, T. Eriksson, and A. Svensson, "Receiver algorithms for OFDM systems in phase noise and AWGN," in *Proc. IEEE PIMRC*, Sep. 2004.
- [17] A. Demir, A. Mehrotra, and J. Roychowdhury, "Phase noise in oscillators: A unifying theory and numerical methods for characterisation," *IEEE Trans. Circuits Syst. I*, vol. 47, no. 5, pp. 655–674, May 2000.
- [18] A. Mehrotra, "Noise analysis of phase-locked loops," *IEEE Trans. Circuits Syst. I*, vol. 49, no. 9, pp. 1309–1316, Sep. 2002.
- [19] D. Petrovic, W. Rave, and G. Fettweis, "Intercarrier interference due to phase noise in OFDM—Estimation and suppression," in *Proc. IEEE VTC Fall*, Sep. 2004, pp. 2191–2195.

- [20] W. Rave, D. Petrovic, and G. Fettweis, "Iterative correction of phase noise in multicarrier modulation," in *Proc. 9th Int. OFDM Workshop*, Sep. 2004.
- [21] S. Weinstein and P. Ebert, "Data transmission by frequency-division multiplexing using the discrete Fourier transform," *IEEE Trans. Commun.*, vol. COM-19, no. 5, pp. 964–967, Oct. 1971.
- [22] S. Mirabbasi and K. Martin, "Classical and modern receiver architectures," *IEEE Commun. Mag.*, vol. 38, no. 11, pp. 132–139, Nov. 2000.
- [23] T. C. W. Schenk, X.-J. Tao, P. F. M. Smulders, and E. R. Fledderus, "On the influence of phase noise induced ICI in MIMO OFDM systems," *IEEE Commun. Lett.*, vol. 9, no. 8, pp. 682–684, Aug. 2005.
- [24] A. Oppenheim and R. Schaffer, *Discrete-Time Signal Processing*. Englewood Cliffs, NJ: Prentice-Hall, 1989.
- [25] A. Mehrotra, "Noise in radio frequency circuits: Analysis and design implications," in *Proc. Int. Symp. Quality Electron. Design*, 2001, pp. 469–476.
- [26] C. Gardiner, *Handbook of Stochastic Methods for Physics, Chemistry and Natural Sciences*. Berlin, Germany: Springer-Verlag, 1994.
- [27] S. M. Kay, *Fundamentals of Statistical Signal Processing*, vol. 1. Englewood Cliffs, NJ: Prentice-Hall, 1998.
- [28] S. Haykin, *Adaptive Filter Theory*, 3rd ed. Englewood Cliffs, NJ: Prentice-Hall, 1996.
- [29] D. Petrovic, W. Rave, and G. Fettweis, "Properties of the intercarrier interference due to phase noise in OFDM," in *Proc. IEEE Int. Conf. Commun.*, 2005, pp. 2605–2610.
- [30] S. Wu and Y. Bar-Ness, "Performance analysis of the effect of phase noise in OFDM systems," in *Proc. IEEE 7th ISSSTA*, Prague, Czech Republic, 2002, pp. 133–138.
- [31] L. Piazza and P. Mandarini, "Analysis of phase noise effects in OFDM modems," *IEEE Trans. Commun.*, vol. 50, no. 10, pp. 1696–1705, Oct. 2002.
- [32] G. Fettweis, M. Löhning, D. Petrovic, M. Windisch, P. Zillmann, and W. Rave, "DIRTY RF: A new paradigm," in *Proc. 16th IEEE PIMRC*, Sep. 2005, vol. 4, pp. 2347–2355.



Denis Petrovic (S'98–M'00) was born in Belgrade, Yugoslavia, in 1976. He received the Dipl.-Ing. degree from the University of Belgrade, Serbia, in 2001 and the Ph.D. degree in electrical engineering from Dresden University of Technology, Dresden, Germany, in 2005.

He was involved in several research projects with California Institute of Technology, Pasadena; Vodafone Chair Mobile Communications Systems, Dresden University of Technology; and Ericsson Eurolab Deutschland, Nueremberg, Germany. He is currently a Research and Development Engineer with Rohde&Schwartz, Munich, Germany, focusing on 3G communications testing systems.



Wolfgang Rave received the Graduate degree of materials science for electrical engineering and the Ph.D. degree from the University of Erlangen-Nuremberg, Nuremberg, Germany, in 1990.

From 1990 to 1992, he was a Research and Development Engineer with AEG, Heilbronn, Germany, where he worked on infrared detectors and readout circuits for the German company. In 1993–1994, he was a Postdoctoral Fellow with the Université Paris-Sud, Orsay, France. He joined the Institute for Solid State and Materials Research, Dresden, Germany, as a Research Scientist in 1995. He joined the Vodafone Chair Mobile Communications Systems, Dresden University of Technology, Dresden, in 1999. His current research interests include orthogonal frequency division multiplexing and MIMO communication techniques, and the influence of nonlinear distortions and their correction by iterative detection and decoding.



Gerhard Fettweis (S'84–M'90–SM'98) received the Ph.D. degree in electrical engineering from Aachen University of Technology, Aachen, Germany, in 1990.

From 1990 to 1991, he was a Visiting Scientist at IBM Almaden Research Center, San Jose, CA, developing signal processing innovations for IBM's disk-drive products. From 1991 to 1994, he was a Scientist with TCSI Inc., Berkeley, CA, responsible for signal processor development projects for mobile phone chip-sets. Since September 1994, he has been the Chair of the Vodafone Chair Mobile Communications Systems, Dresden University of Technology, Dresden, Germany. He cofounded Systemonic in 1999, successfully acquired by Philips Semiconductor in December 2002, where he is currently a Chief Scientist. His current research interests include new wireless communication systems for cellular and short-range networks, and their hardware/software implementation.